Original Article

Study on the pathogenesis of idiopathic pediatric acute pancreatitis by combining intestinal microbiome and metabolome

Feng Liu[1,2], Ying Sun[3], Jizhong Wang[2], Jianghua Zhan[1,4]

[1]Clinical School of Paediatrics, Tianjin Medical University, Tianjin, China; [2]Department of Emergency and Trauma Surgery, Tianjin Children's Hospital, Tianjin, China; [3]Department of Anesthesiology, Tianjin First Central Hospital, Tianjin, China; [4]Department of General Surgery, Tianjin Children's Hospital, Tianjin, China

Contributions: (I) Conception and design: J Zhan; (II) Administrative support: J Zhan; (III) Provision of study materials or patients: F Liu; (IV) Collection and assembly of data: Y Sun, J Wang; (V) Data analysis and interpretation: F Liu, Y Sun; (VI) Manuscript writing: All authors; (VII) Final approval of manuscript: All authors.

Correspondence to: Jianghua Zhan, MD. Clinical School of Paediatrics, Tianjin Medical University, 225 Machang Road, Hexi District, Tianjin 300070, China; Department of General Surgery, Tianjin Children's Hospital, Tianjin, China. Email: zhanjianghuatj@163.com.

Background: Idiopathic pediatric acute pancreatitis (IPAP) represents a significant health threat to children and adolescents, yet its underlying pathogenesis remains poorly understood, necessitating further research to elucidate its mechanisms. This study aims to explore the roles of intestinal microbiota, short-chain fatty acids (SCFAs), and serum metabolites in the pathogenesis of IPAP, as well as to assess the therapeutic potential of acetic acid intervention in this condition.

Methods: Fecal and serum samples from 22 cases of IPAP (excluding biliary origin) and 10 healthy controls were collected and analyzed. Intestinal microbial was characterized using 16S ribosomal RNA (16S rRNA) sequencing, while SCFAs and serum metabolites were quantified by liquid chromatography-tandem mass spectrometry (LC-MS/MS). Omics analysis was employed to identify microbial-metabolite regulation and regulatory networks and potential disease biomarkers. To evaluate the therapeutic efficacy of acetic acid in acute pancreatitis (AP), AP was induced in animal models by intraperitoneal injection of caerulein (50 μg/kg; once daily for seven days), followed by oral administration of acetic acid (10 mL/kg, once daily) in 4-, 6-, and 8-week models. Pancreatic and ileum tissues were examined for histopathological changes, serum enzymes levels, and intestinal barrier integrity.

Results: The results of 16S rRNA sequencing revealed significant differences in the composition and abundance of intestinal microbial communities between the control (Con) and IPAP groups. Pathogenic bacteria, such as *f_Tannerellaceae* and *c_Bacteroidia*, as well as certain symbiotic bacteria, were significantly enriched in the IPAP group. SCFAs metabolome analysis indicated that acetic acid, as a key intermediate metabolite, may play a regulatory role in the pathogenesis of IPAP. The construction of a microbial-metabolite regulatory network demonstrated that microorganisms such as *g_Monoglobus* and *g_Morganella* were closely associated with SCFAs, including acetic acid, suggesting that the development of IPAP is influenced by upstream and downstream regulatory mechanisms. Furthermore, significant associations were identified between serum metabolites and gut microbes. For instance, (4E,15E)-bilirubin and creatinine showed significant positive correlations with *g_Bacteroides* ($P<0.01$). Similarly, 1,2-ethanediol monoricinoleate was significantly positively correlated with *g_Hungatella* ($P<0.01$), while pubescenol and tecastemizole were significantly positively correlated with *g_Parabacteroides* ($P<0.01$). Animal experiments demonstrated that pancreatic and intestinal tissue damage was alleviated to varying degrees following treatment. Compared to the disease model group, the acetic acid treatment group exhibited significantly reduced serum levels of D-lactic acid, amylase, and lipase, along with a significantly increased positive staining surface density of intestinal barrier proteins (occludin, claudin-1, and ZO-1).

Conclusions: Intestinal flora, SCFAs and serum metabolites were significantly altered in IPAP, and the interaction regulated the development of IPAP. Acetic acid can effectively intervene the occurrence of IPAP.

Keywords: Idiopathic pediatric acute pancreatitis (IPAP); acetic acid; gut microbiome; short-chain fatty acids (SCFAs); serum metabolome

Submitted Dec 10, 2024. Accepted for publication Mar 27, 2025. Published online May 21, 2025.
doi: 10.21037/tp-2024-571
View this article at: https://dx.doi.org/10.21037/tp-2024-571

Introduction

Background

Idiopathic pediatric acute pancreatitis (IPAP) is a sudden, severe digestive disorder of unknown etiology. Several possible risk factors, including biliary tract disease, drug use, systemic disease, abdominal trauma, metabolic disorders, and inborn metabolic defects, are known to exist in current studies, and the prevalence of risk factors varies in children of different ages (1). IPAP not only affects a child's pancreatic function, but may also affect multiple systems throughout the body. There is an urgent need for effective means to analyze its pathogenesis and develop treatment strategies.

Rationale and knowledge gap

In recent years, with the rapid development of microbiomes and metabolomics technologies, the role of gut microbiota in a variety of diseases has been gradually revealed. The gut microbiota is not only involved in digestive and metabolic processes, but also has a profound impact on systemic health by regulating immune responses and maintaining gut barrier function (2). Especially in the study of acute pancreatitis (AP), the role of gut microbiota has attracted extensive attention. The occurrence of AP is related to intestinal microbial community. Inflammation triggered by AP increases intestinal permeability, leading to damage of the intestinal mucosal barrier and bacterial translocation, which may contribute to infection-related complications (3). While numerous studies on adult AP have focused on the observation and modulation of intestinal flora (4,5), research on pediatric AP remains limited, with insufficient evidence to draw definitive conclusions. Whether the occurrence of IPAP is related to the disorder of intestinal microbiome and whether the derived regulatory relationship affects the development of the disease are worthy of further study and discussion.

Intestinal microorganisms produce metabolites through metabolic activities and establish close interaction with the host. Studies have revealed significant alterations in serum metabolites among patients with chronic pancreatitis. These differences in metabolic profiles have been analyzed using liquid chromatography-tandem mass spectrometry (LC-MS/MS) technology to identify potential diagnostic biomarkers for chronic pancreatitis (6). *Clostridium butyricum* alleviates AP-induced lung injury by regulating fatty acid metabolism (7). This evidence indicated the important role of gut microbiome in AP. In this context, the combined application of gut microbiome and metabolomics in the study of IPAP has become a necessary and promising research strategy. For this study, we hypothesize that dysregulation of the gut microbiome and alterations in derived metabolites play a key role in the pathogenesis of IPAP.

Objective

In this study, stool and serum samples were collected

Highlight box

Key findings

- Intestinal flora, short-chain fatty acids (SCFAs) and serum metabolites were significantly altered in idiopathic pediatric acute pancreatitis (IPAP), and the interaction regulated the development of IPAP. Acetic acid can effectively intervene the occurrence of IPAP.

What is known and what is new?

- The pathogenesis of IPAP may be related to the changes of intestinal microbes and metabolites, but the specific mechanism is not clear.
- Acetic acid is a key regulator of IPAP, which can effectively reduce pancreatic and ileum damage. Intestinal flora, SCFAs and serum metabolites were significantly altered in IPAP, and the interaction regulated the development of IPAP.

What is the implication, and what should change now?

- This study highlights potential therapeutic targets for IPAP, suggesting interventions such as probiotics or fecal microbiota transplantation to modulate the gut microbiota, restore microbial balance, and potentially slow disease progression. Furthermore, novel therapeutic strategies could be developed by targeting specific metabolites or identified metabolic pathways.

from 22 children with IPAP and 10 healthy controls. The composition and alterations of the intestinal microbiota were analyzed using 16S ribosomal RNA (16S rRNA) gene sequencing, while metabolome differences were assessed by LC-MS/MS. The obtained data were integrated and analyzed to construct a comprehensive regulatory network centered on intestinal microbes in IPAP. This approach aimed to explore the intrinsic relationships within intestinal microecology and to evaluate the effects of acetic acid on IPAP, which providing novel insights and perspectives into the pathogenesis of IPAP. Additionally, in terms of clinical significance, this study highlights potential therapeutic targets for IPAP, suggesting interventions such as probiotics or fecal microbiota transplantation to modulate the gut microbiota, restore microbial balance, and potentially slow disease progression. Furthermore, novel therapeutic strategies could be developed by targeting specific metabolites or identified metabolic pathways. We present this article in accordance with the ARRIVE reporting checklist (available at https://tp.amegroups.com/article/view/10.21037/tp-2024-571/rc).

Methods

Clinical sample collection

This study was conducted in accordance with the Declaration of Helsinki and its subsequent amendments. The Medical Ethics Committee of Tianjin Children's Hospital approved this study (No. W-2024-022) and waived the requirement for written informed consent, in line with local guidelines. Children with IPAP (excluding biliary pancreatitis) admitted to Tianjin Children's Hospital between October 2022 and March 2023 were recruited. Based on the revised Atlanta classification, all children met the diagnostic criteria for AP. Children with severe autoimmune diseases, hematologic disorders, significant impairment of liver, lung, kidney, or other organ functions, severe cardiovascular or cerebrovascular diseases, poor treatment compliance, or serious complications during treatment were excluded. Healthy controls were also recruited. Both children and healthy controls who had received antibiotics or probiotics within four weeks prior to admission were excluded.

Fecal and blood samples were collected from 22 children with IPAP and 10 healthy controls. Two fresh fecal samples and one fresh blood sample were obtained from each participant. Fecal samples were collected in sterile sample tubes, placed in an insulated box with ice packs, and promptly transported to the laboratory, where they were stored at −80 ℃ for subsequent sequencing analysis and metabolite detection. Blood samples were collected within 24 hours of admission after an 8-hour fasting period, and serum was separated by centrifugation.

16S rRNA sequencing analysis of the intestinal microbiome

Genomic DNA was extracted using the MagPure Soil DNA LQ Kit (Magen, China) and stored at −20 ℃ following quality assessment. The extracted DNA was used as a template to amplify the V3-V4 region of the 16S rRNA gene with the primers 343F (5'-TACGGRAGGCAGCAG-3') and 798R (5'-798RAGGGTATCTAATCCT-3') (8) for bacterial diversity analysis. Polymerase chain reaction (PCR) products were visualized by gel electrophoresis, purified, re-amplified, and re-purified. Subsequently, the products were quantified using Qubit and sequenced on the Illumina NovaSeq 6000 platform (Aglient, USA), generating 250 bp paired-end reads. Sequencing was conducted by Shanghai OE Biotech Co., Ltd. (Shanghai, China). All samples were processed in a single sequencing run. Sequence data were normalized using QIIME2 (9), and low-quality sequences and chimeras were removed using DADA2 (10). Primer sequences were trimmed using Cutadapt, while DADA2 was employed for quality control (QC). QIIME2 was used for representative sequence selection, taxonomic annotation, and α/β diversity analysis. Differential analyses were performed using *T*-test/Wilcoxon test in R and Linear discriminant analysis Effect Size (LEfSe) for species abundance analysis.

LC-MS/MS analysis of intestinal SCFAs metabolome

Fecal samples were mixed with 300 μL of acetonitrile, ground in a −20 ℃ dish, and subjected to ultrasound treatment. The mixture was centrifuged, and the supernatant was diluted fivefold. Subsequently, 80 μL of the diluted supernatant was transferred to a vial. Derivatization reagents were added, and the mixture was incubated at 40 ℃, cooled, filtered, and stored at −80 ℃. QC samples were prepared by pooling equal volumes of each sample. Throughout the LC-MS/MS analysis, QC samples were injected at regular intervals. Peak areas were normalized to internal standard and QC samples, and the missing values are filled with half of the matrix minimum. Multiple tests

were performed by Benjamini-Hochberg method.

A total of 12 SCFAs were detected using LC-MS/MS. Chromatographic conditions included a 1 µL injection volume and a flow rate of 0.35 mL/min with gradient elution. Mass spectrometry (MS) were set as follows: curtain gas 35 psi, collision gas at medium, ion spray voltage at –4,500 V, and ion source temperature at 450 ℃. Transitions were automatically identified using MRMPro software and subsequently manually inspected and corrected.

Serum metabolome LC-MS/MS analysis

The serum was thawed in an ice-water bath, and 100 µL was transferred to an Eppendorf (EP) tube. Subsequently, 400 µL of a methanol-acetonitrile mixture (2:1, v/v) was added, followed by vortexing and sonication for 10 min. The mixture was then stored at –40 ℃ for 2 hours. After centrifugation at 13,000 rpm for 20 minutes, 150 µL of the supernatant was collected, filtered, transferred to an LC vial, and stored at –80 ℃. QC sample was prepared by pooling equal volumes of each extract. Throughout the LC-MS/MS analysis, QC samples were injected at regular intervals. Peak areas were normalized to the internal standard and QC samples, and the missing values are filled with half of the matrix minimum. Multiple tests were performed by Benjamini-Hochberg method.

Metabolites were detected using LC-MS/MS with the following parameters: a 3 µL injection volume, a flow rate of 0.35 mL/min, and gradient elution using mobile phases A and B. MS conditions included a capillary temperature of 320 ℃, an auxiliary gas temperature of 350 ℃, and a mass range of 70–1,050 m/z in both positive and negative ion modes. Data were processed using Progenesis QIv3.0 software. Compound identification was based on retention time, mass-to-charge ratio, fragmentation patterns, and isotope distribution, with reference to the HMDB, Lipidmaps, METLIN, and LuMet-Animal 3.0 databases.

Animal experiments

Thirty 4-week-old C57BL/6J male mice were purchased from Beijing Sibeifu Laboratory Animal Technology Co., Ltd. (Beijing, China), with laboratory animal production license number: SCXK (Beijing, China) 2022-0006, and laboratory animal qualification certificate number: 111423220100018067. This experiment was performed in compliance with Chinese guidelines on animal care and use. All animals were housed in a specific pathogen free facility under standardized conditions. The mice were acclimated for 1 week prior to the experiment and maintained on a standardized diet with ad libitum access to water. Environmental conditions included a room temperature of 20–26 ℃, relative humidity of 40–70%, and a 12-hour light/dark cycle. Additionally, bedding was replaced at regular intervals for all mice. The experimental protocol was approved by the Animal Ethics Committee of Tianjin Jinke Bona Biotechnology Co., Ltd. (No. GENINK-20240020). Before inducing the AP model, all mice were fasted for 18 hours. The mice were then randomly divided into five groups. The control group received no treatment and was fed normally. The model group was administered intraperitoneal injection of caerulein at a dose of 50 µg/kg once daily for seven consecutive days. The treatment group received acetic acid solution via oral gavage 24 hours after modeling, with a dose of 10 mL/kg administered once daily for 4, 6, and 8 weeks, respectively. Mice were euthanized 24 hours after modeling or treatment, and blood samples were immediately collected. Serum was separated and stored at –80 ℃ for subsequent analysis of serum amylase (AMS), D-lactate (D-LA), and lipase within 48 hours. The pancreas and ileum were then harvested, and residual blood was removed using ice-cold saline. One portion of the tissues was fixed in 10% formalin solution, while the other portion was stored at –80 ℃ for further experiment.

Serum testing

Mouse AMS, mouse D-LA and mouse lipase enzyme-linked immunosorbent assay (ELISA) kits were used to measure the levels of serum AMS, lipase and D-LA.

Histological analysis

The pancreas and ileum samples were fixed in 20 volumes of fixative, embedded in paraffin, sectioned, and stained with hematoxylin-eosin (HE).

Immunofluorescence

Immunofluorescence staining was performed to detect occludin, claudin-1, ZO-1, in order to assess inflammation in the pancreas and ileum. Tissue samples were dewaxed, subjected to antigen retrieved, and blocked with bovine serum albumin. Subsequently, the samples were incubated with primary antibodies against occludin, claudin-1, ZO-1, followed by incubation with a secondary antibody. Nuclei were counterstained with 4',6-diamidino-2-phenylindole,

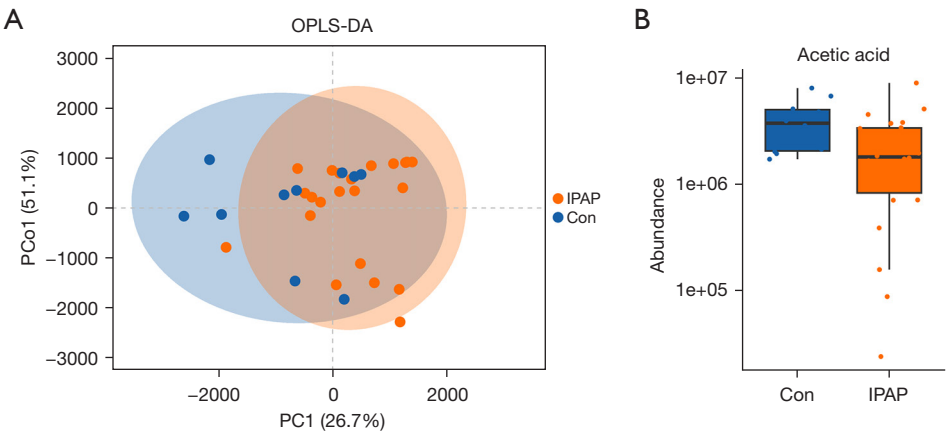

Figure 1 Fecal short-chain fatty acid abundance statistics of control and IPAP groups. (A) OPLS-DA of fecal short-chain fatty acids between control and IPAP groups. (B) Acetic acid distribution box diagram of fecal between control and IPAP groups. Con, control group; IPAP, idiopathic pediatric acute pancreatitis; OPLS-DA, orthogonal partial least squares discriminant analysis.

and images were acquired using a fluorescence microscope.

Statistical analysis

The omics data was statistically analyzed using R (version 4.1.0) and Python (version 3.8). For 16S rRNA sequencing data, differential abundance analysis was performed using the Wilcoxon rank-sum test or *t*-test, and P values were adjusted for multiple comparisons using the Benjamini-Hochberg false discovery rate (FDR) method. Sensitivity to sequencing depth was assessed through rarefaction analysis. For metabolomics data, univariate tests (e.g., *t*-test, Mann-Whitney *U* test) were applied, and Benjamini-Hochberg was employed to control for multiple comparisons. Multivariate analyses, such as partial least squares-discriminant analysis, were validated using permutation test (n=1,000). Sensitivity analysis was conducted by iteratively removing subsets of samples and testing alternative normalization methods.

Data were analyzed using SPSS26.0 (Chicago, IL, USA). The Shapiro-Wilk test was used to test the type of parameter distribution, and the measurement data that conforms to the normal distribution were expressed as $\bar{x}\pm s$. Comparisons between groups were performed using independent sample *t*-test, one-way analysis of variance was performed on the three groups of standard distribution data, and *post hoc* least significant difference (LSD) test was performed. $P<0.05$ indicated statistically significant difference.

Results

Acetate is a key regulator of IPAP

To characterize the SCFAs composition in IPAP, we performed a targeted metabolome analysis of SCFAs. A total of seven SCFAs were detected in all fecal samples, including acetate, propionate, butyrate, valerate, caproate, isobutyrate, and isovalerate. Orthogonal partial least squares discriminant analysis (OPLS-DA) revealed distinct differences in SCFAs composition between the control group (Con) and disease group (IPAP) (*Figure 1A*). The variable importance in projection value of acetic acid was 2.60, significantly higher than those of other metabolites, indicating that acetic acid was the primary contributor to distinguishing the Con group from the IPAP group. The acetic acid content in the Con group was significantly higher than that in IPAP group (*Figure 1B*). As a key intermediate metabolite, acetic acid has been reported to play a regulatory role in AP through intestinal flora interactions (11). Therefore, acetic acid may be involved in the disease regulation of IPAP and could be used as a biomarker for further investigation.

Intestinal microbiome and short-chain fatty acid (SCFA) changes synergistically affect IPAP

To characterize the intestinal flora of IPAP, we analyzed all fecal samples using 16s rRNA sequencing. A total of

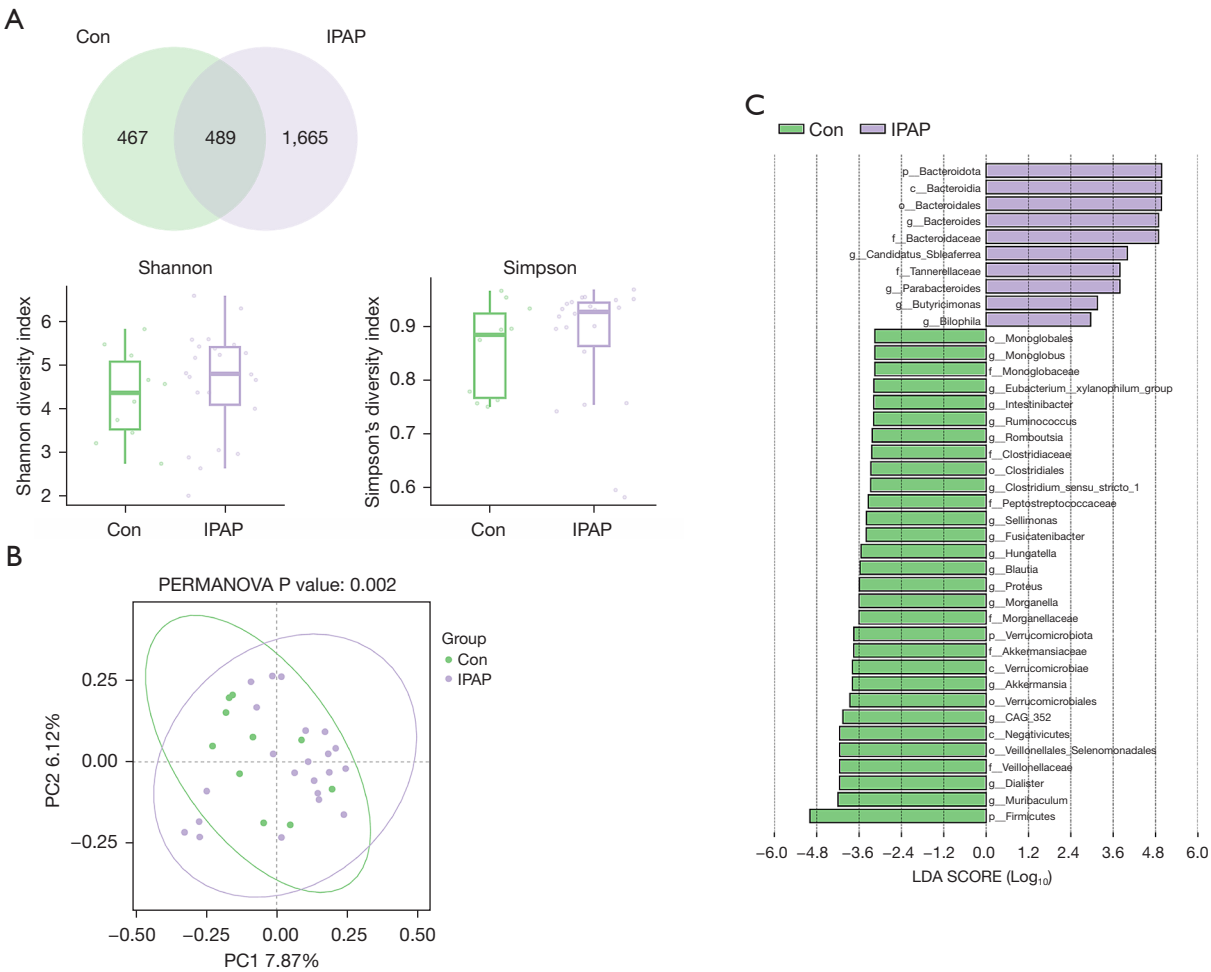

Figure 2 The difference of microbial composition and structure between control and IPAP groups. (A) ASVs Venn diagrams identified in both groups. The Y coordinate is the Shannon diversity index and Simpson's diversity index. (B) PCoA presentation of ASVs. (C) LEfSe analysis of ASVs. ASV, amplicon sequence variant; Con, control group; IPAP, idiopathic pediatric acute pancreatitis; LDA, linear discriminant analysis; LEfSe, Linear discriminant analysis Effect Size; PCoA, principal coordinate analysis.

27 phyla, 52 classes, 126 orders, 200 families, 385 genera, and 706 species were identified. Compared to the Con group, the species richness and diversity of the IPAP group were increased (*Figure 2A*). Principal coordinate analysis (PCoA) revealed a distinct separation between the two groups (*Figure 2B*), indicating significant alterations in intestinal flora associated with IPAP. Linear discriminant analysis (LDA) coupled with effect size measurements was used to analyze differences in the microbial abundance between the two groups (*Figure 2C*). A total of 40 species with significant differences were identified (P<0.05, LDA score >2). Among these 10 species were significantly enriched in the IPAP group, while 30 species showed significantly increased abundance in the Con group, accounting for 5.9% of the total microbial abundance. Among the 40 differentially abundant microorganisms, *g_Morganella*, *g_Proteus*, *g_Dialister* and *f_Veillonellaceae* were significantly enriched in Con group. In IPAP group, *f_Tannerellaceae*, *g_Parabacteroides*, *c_Bacteroidia*, and *g_Butyricimonas* contributed the most to the observed differences. Notably, most of the microorganisms enriched in IPAP group were pathogenic or symbiotic bacteria, such as *f_Tannerellaceae* and *c_Bacteroidia*. In contrast, beneficial bacteria, including *g_Monoglobus*, *g_Dialister*, were predominantly present in Con group. The top 100 amplicon sequence variants (ASVs) based on abundance were selected for clustering analysis

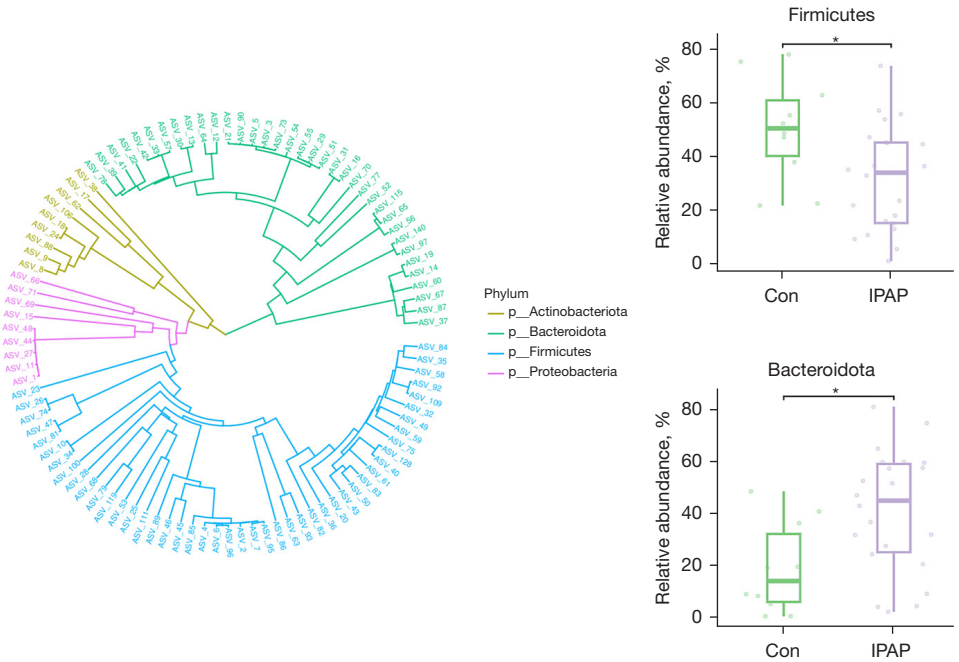

Figure 3 Classification of ASVs at phylum level and characteristic microbiological analysis based on Wilcoxon test. *, P<0.05. ASV, amplicon sequence variant; Con, control group; IPAP, idiopathic pediatric acute pancreatitis.

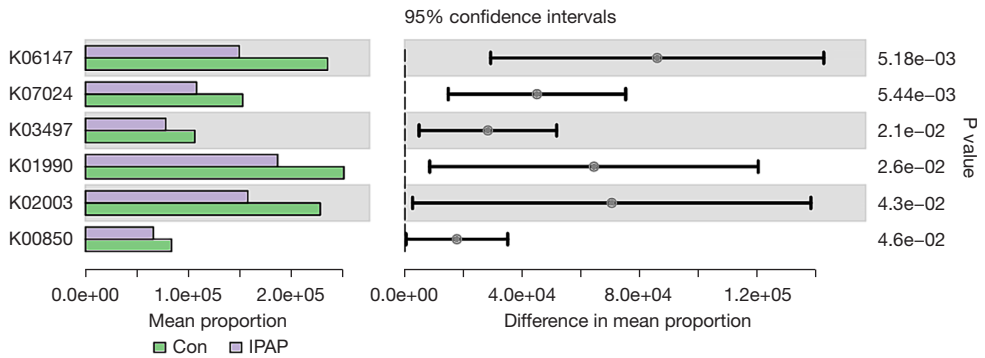

Figure 4 Functional enrichment of ASVs. ASV, amplicon sequence variant; Con, control group; IPAP, idiopathic pediatric acute pancreatitis.

(*Figure 3*). At the phylum level, the most abundant taxa were *p_Firmicutes*, followed by *p_Bacteroidota*. The abundance of *p_Firmicutes* in the Con group was significantly higher than that in the IPAP group.

Based on the statistical analysis of Kyoto Encyclopedia of Genes and Genomes (KEGG) functional pathways using the *t*-test, the top six most abundant pathways included K06147 (ABCB-BAC; ATP-binding cassette, subfamily B, bacterial), K07024 (SPP; sucrose 6-phosphatase), K03497 (SPP; sucrose 6-phosphatase), K01990 (ABC-2.A; ABC-2 type transport system ATP-binding protein), K02003 (ABC.CD.A; putative ABC transport system ATP-binding protein), K00850 (pfkA, PFK; 6-phosphofructokinase 1) (*Figure 4*). K06147, K01990 and K02003 belong to the ABC transporter gene family, which is typically involved in the excretion of toxic substances and the import of nutrients (12). Previous study has shown that K06147 expression in the gut was significantly reduced in patients with rectal cancer (13); while K06147, K01990 and K02003 were found to be enriched in the gut microbiota of corsac foxes, potentially aiding their adaptation to harsh environments (14). 6-phosphofructokinase 1 plays a role in carbohydrate

metabolism and the tricarboxylic acid (TCA) cycle, and its activity may be positively regulated by *g_Lactobacillus* (15). It has been widely reported that *g_Lactobacillus* is beneficial for disease treatment, particularly in mitigating chronic inflammation. For example, in the context of colon cancer, *g_Lactobacillus* has been shown to promote apoptosis through the production of metabolic substances and to inhibit tumorigenesis (16).

The Spearman correlation algorithm was employed to analyze the correlation between the SCFAs and the microbiome. The distribution of the first principal component revealed a correlation coefficient of 0.37 between the two omics datasets, indicating a moderate correlation (*Figure 5A*). In order to further explore the relationship between intestinal microbes and SCFAs, we identified the key features associated with the model components. The correlation distribution (*Figure 5B*) revealed that acetic acid, butyric acid, *g_Monoglobus* and *g_Morganella* were the most highly correlated and significant SCFAs and microorganisms. The frequency of each differential feature in the two omics datasets was calculated, and nodes with high association frequencies were identified (*Figure 5C*). Key microbiome nodes include *g_Monoglobus*, *g_Ruminococcus*, *g_Hungatella* and *g_Morganella*, while the SCFAs nodes comprised acetic acid and butyric acid. SCFAs are metabolites of intestinal microorganisms and play a collaborative role in maintaining intestinal homeostasis (17). In the association network (*Figure 5D*), these features also exhibited strong interconnections. Notably, acetic acid showed significant correlations with *g_Monoglobus* and *g_Morganella* (P<0.01) (*Figure 5E*). Previous study has demonstrated that acetate, a metabolite produced by intestinal flora during influenza virus infection, can enhance type I interferon production through the NLRP3 pathway, thereby conferring resistance to viral infection (18).

Intestinal microbiota is associated with changes in serum metabolome

Next, we used LC-MS/MS to analyze the metabolic profiles of serum samples from the two groups to explore the characteristics of the serum metabolome in children with IPAP. A total of 4,244 metabolite datasets were annotated, with amino acids, peptides, and analogues (10.82%), fatty acids and conjugates (8.62%), and fatty acid esters (3.25%) representing the largest proportions in the secondary classification (*Figure 6A*). Principal component analysis (PCA) showed a clear separation between the Con group and the IPAP group, indicating significant differences in metabolites (*Figure 6B*). Metabolites with significant enrichment differences between the two groups included fatty acids and conjugates, glycerophosphocholines, amino acids, peptides, and analogues (*Figure 6C*). The altered metabolic pathways involved fatty acid biosynthesis, choline metabolism in cancer, fatty acid degradation, arginine and proline metabolism, and arachidonic acid metabolism (*Figure 6D*). These changes suggest that IPAP leads to increased energy and metabolic expenditure. Pathways such as fatty acid metabolism and choline metabolism are involved in the regulation of acute inflammation (19,20).

Therefore, we conducted a joint analysis to explore the relationship between the gut microbiome and the serum metabolome. The correlation results among components (*Figure 7A*) demonstrated a strong correlation between the two omics datasets (correlation coefficient: 0.89). By constructing the microbial-serum metabolite network (*Figure 7B*), we identified *g-Bacteroides*, *g-Hungatella*, *g_Parabacteroides*, *g_Morganella* and *g_Dialister* as the nodes with the highest connectivity, primarily involved in forming these relationships. Specifically, (4E,15E)-bilirubin, creatinine, and D-fructose showed positive correlations with *g_Bacteroides* (P<0.01). Similarly, 1,2-ethanediol monoricinoleate, bis(2-ethylhexyl) phthalate, and 4-dodecylbenzenesulfonic acid were positively correlated with *g_Hungatella* (P<0.01). Additionally, pubescenol, tecastemizole, and (4E,15E)-bilirubin exhibited positive correlations with *g_Parabacteroides* (P<0.01) (*Figure 7C*). Excessive accumulation of bilirubin in the blood can lead to jaundice or neurological damage. Previous study has found that bilirubin reductase (BilR), derived from intestinal microorganisms, can reduce bilirubin to urobilinogen (21). In addition, intestinal flora can metabolize fructose to produce acetate, which participates in glutamine synthesis, thereby promoting tumor cell growth (22).

Acetic acid can treat AP in mice

To validate the hypothesis that acetic acid alleviates IPAP, we established a mouse model of AP using caerulein. Histological analysis (*Figure 8A*) revealed damage to both the ileum and pancreas in the disease model group. The ileum exhibited structural abnormalities, including mucosal layer disruption and partial villous edema. Pancreatic tissue displayed structural disorganization, characterized by acinar cell degeneration and necrosis, islet atrophy, and inflammatory cell infiltration. Following acetic acid

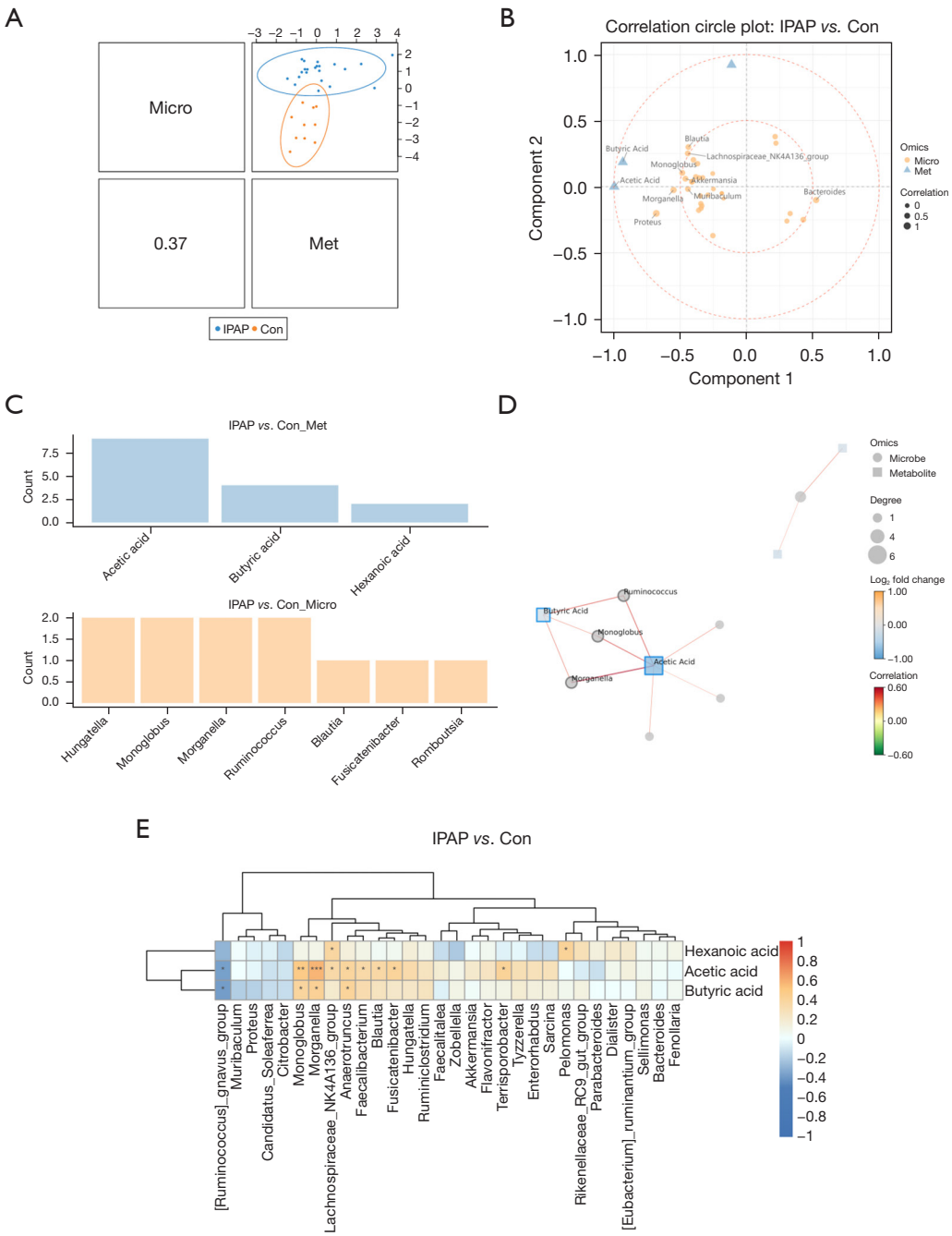

Figure 5 The relationship between microorganisms and short-chain fatty acids. (A) The correlation coefficient between the two omics. (B) Correlation circle plot of microorganisms and metabolites. (C) Significantly different characteristics of metabolites and microorganisms. (D) Characteristic metabolites and microbial correlation networks. (E) Correlation heatmap of characteristic metabolites and microorganisms. *, P<0.05; **, P<0.01; ***, P<0.001. Con, control group; IPAP, idiopathic pediatric acute pancreatitis; Met, metabolite; Micro, microorganism.

treatment at different time, the damage to the ileum and pancreatic tissue in the diseased mice was alleviated to varying degrees. Notably, the 6- and 8-week treatment groups showed significant tissue recovery, with levels comparable to those of the control group. ELISA results showed (*Figure 8B*) that, compared to the control group,

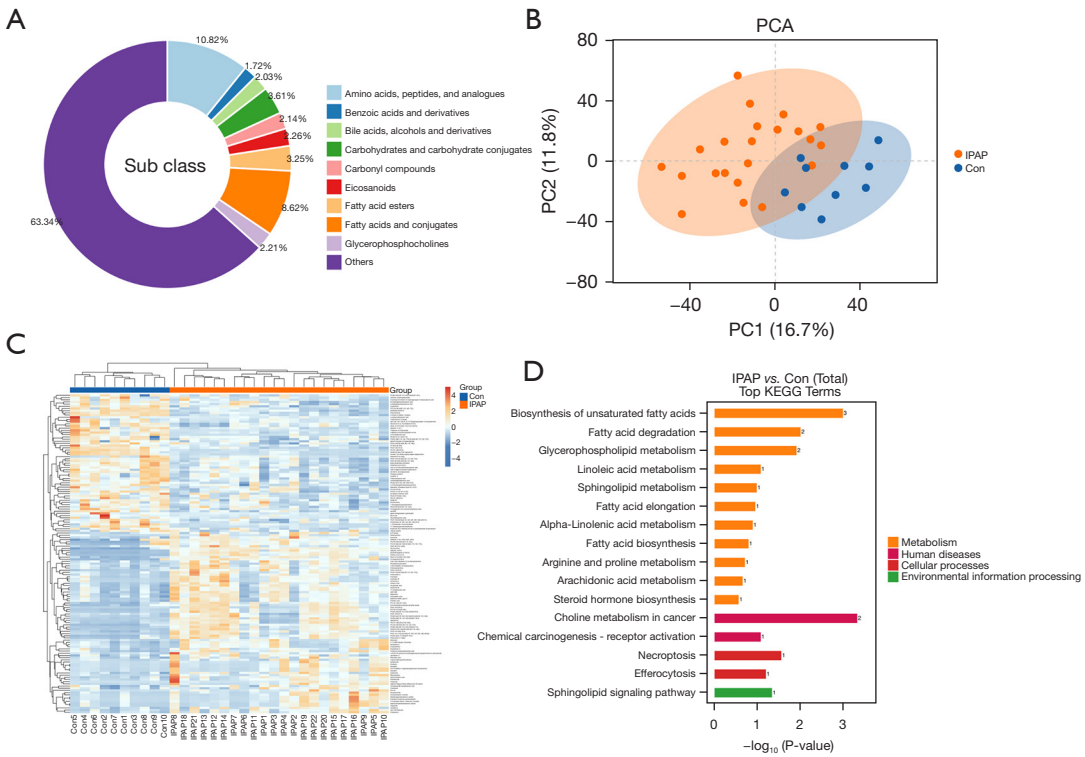

Figure 6 Serum metabolite analysis between the two groups. (A) Classification of identified serum metabolites. (B) PCA analysis between the two omics. (C) Heatmap of serum metabolite distribution. (D) Serum metabolite KEGG function enrichment. Con, control group; IPAP, idiopathic pediatric acute pancreatitis; KEGG, Kyoto Encyclopedia of Genes and Genomes; PCA, principal component analysis.

serum levels of D-LA, AMS and lipase were significantly elevated in the disease model group (P<0.001). In contrast, these levels were significantly reduced in the treatment group (P<0.001), particularly in the 6- and 8-week treatment groups. Immunofluorescence analysis of intestinal barrier proteins, including occludin, claudin-1 and ZO-1, revealed that the positive staining surface density in the disease model group was significantly lower than that in the control group (*Figure 9*), indicating impaired intestinal barrier function. The treatment group showed gradual improvement in barrier function with increasing treatment duration.

Discussion

In this study, we conducted an integrated analysis of changes in the intestinal microbiome, fatty acids, and serum metabolome with IPAP. This approach enabled the establishment of relevant regulatory networks and the identification of key regulatory nodes. The effect of acetic acid on IPAP was verified by animal experiments, providing new insights for the etiological diagnosis and treatment of IPAP.

The SCFAs metabolome elucidated the intestinal metabolic alterations in IPAP by targeting the dynamic changes of characteristic SCFAs. Most of the monitored SCFAs were present at higher levels in the Con group, where they play an important role in regulating the intestinal environment through oxidative energy supply, anti-inflammatory and anti-tumor functions, and maintenance of the intestinal mucosal barrier (17). Previous study has demonstrated that SCFAs can improve colon damage caused by chronic pancreatitis, rebuild barrier function, and protect pancreatic tissue (23). Notably, the acetic acid content was significantly elevated in the Con group, suggesting its potential importance in maintaining intestinal homeostasis.

Compared to the control group, the intestinal flora significantly enriched in IPAP included *f_Tannerellaceae*, *c_Bacteroidia*, *g_Butyricimonas* and *g_Parabacteroides*. *f_Tannerellaceae* has been proved to contribute to gastrointestinal disorders such as diarrhea, inhibit the immune system, and then induce pathogen infection (24).

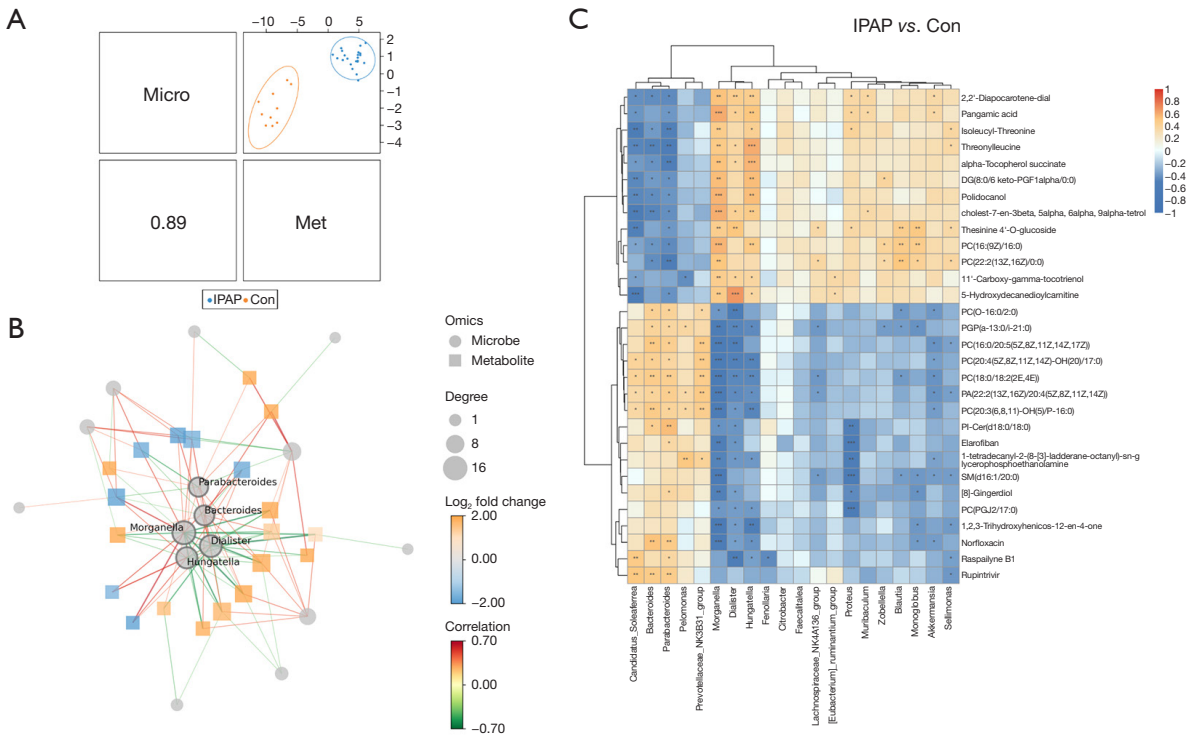

Figure 7 Relationship between serum metabolites and microorganisms. (A) The correlation coefficient between the two omics. (B) Characteristic metabolites and microbial correlation networks. (C) Heatmap of the correlation between the two omics. *, P<0.05; **, P<0.01; ***, P<0.001. Con, control group; IPAP, idiopathic pediatric acute pancreatitis; Met, metabolite; Micro, microorganism.

c_Bacteroidia is obviously enriched in the intestines of patients with AP, and its overgrowth can lead to the change of intestinal barrier function and the impairment of immune function (25). In studies on esophageal cancer, *g_Butyricimonas* has been found to be abundant in cases of recurrent esophageal cancer and may become a key microorganism in predicting postoperative recurrence (26). In addition, *g_Butyricimonas* is also a major microbe in the gut of ulcerative colitis patients who smoke (27). Liu *et al.* investigated the effects of heavy metal arsenic exposure on normally fed mice and observed a significant increase in the relative abundance of *g_Butyricimonas* and *g_Bacteroides* in the gut, whereas no significant changes were detected in mice fed a high-fat diet. This alteration was associated with liver and kidney damage. These findings suggest that gut microbiota responses to adverse factors vary among individuals, leading to differences in disease risk (28). This interesting difference is also evident in our study. Previous research has shown that *g_Parabacteroides* plays an important role in alleviating AP by reducing neutrophil infiltration and producing acetic acid (11). However, in this study, *g_Parabacteroides* was significantly enriched in group IPAP, while its abundance was notably lower in Con group. Pediatric AP differs from adult AP in that it is less induced by excessive alcohol consumption and biliary tract disease and is more often idiopathic. Population differences may affect the diversity and abundance expression of intestinal microbe, leading to distinct disease response patterns. Another notable difference from previous studies involves *g_Morganella*. In an important study, indolimines, a family of small molecule genotoxins derived from *g_Morganella*, were identified for the first time, which can cause DNA damage and lead to the exacerbation of colon tumors (29). In this study, the relative abundance of *g_Morganella* in Con group was significantly higher than that in group IPAP. *g_Morganella* is an opportunistic pathogen widely distributed in the human gut, typically existing in a symbiotic state but has the potential to cause a variety of infections when immune function is compromised. The existence of such differences is not accidental, and more research is needed to determine the reasons. In addition, *g_Monoglobus* and *g_Dialister* were also significantly enriched in the control

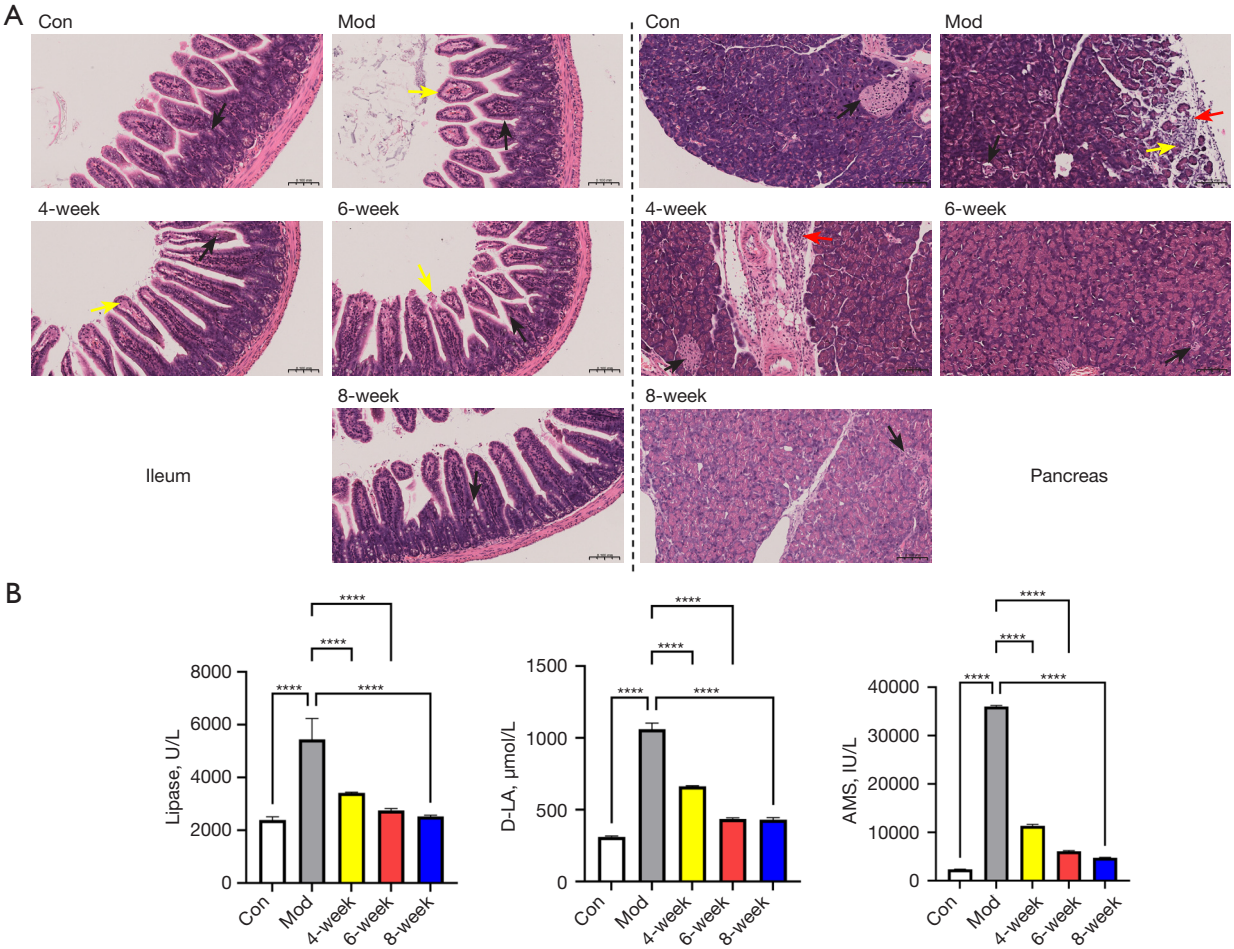

Figure 8 Pathological analysis of pancreas and ileum in mice. (A) HE analysis of pancreas and ileum. The scale is 0.100 mm. Ileum Con: the overall structure of the ileal tissue is basically normal, and the mucosal layer is also basically normal. Goblet cells can be seen (as indicated by the black arrows). Ileum Mod: the overall structure of the ileal tissue is abnormal, the mucosal layer is abnormal, and some villi are edematous (as indicated by the yellow arrow), and goblet cells can be seen (as indicated by the black arrow). Ileum 4-week: the overall structure of the ileal tissue is slightly abnormal, the mucosal layer is abnormal, and some villi are slightly edematous (as indicated by the yellow arrow), and goblet cells can be seen (as indicated by the black arrow). Ileum 6-week: the overall structure of the ileum tissue is slightly abnormal, the mucosal layer is abnormal, and some mucosal epithelium has fallen off (as indicated by the yellow arrow), and goblet cells can be seen (as indicated by the black arrow). Ileum 8-week: the overall structure of the ileal tissue is basically normal, and the mucosal layer is also basically normal. Goblet cells can be seen (as indicated by the black arrows). Pancreas Con: the overall structure of the pancreatic tissue is basically normal, and pancreatic acini and islets can be seen (as indicated by the black arrows). Pancreas Mod: the overall structure of the pancreatic tissue is abnormal, with pancreatic acini and islets visible. Some pancreatic acini undergo degeneration and necrosis (as indicated by the yellow arrows), and islets atrophy (as indicated by the black arrows). Pancreas 4-week: the overall structure of the pancreatic tissue is slightly abnormal. Pancreatic acini and islets can be seen (as indicated by the black arrows), and inflammatory cell infiltration can be observed within the tissue (as indicated by the red arrows). Pancreas 6-week: the overall structure of the pancreatic tissue is slightly abnormal, with pancreatic acini and islets visible, and islets atrophy (as indicated by the black arrows); pancreas 8-week: the overall structure of the pancreatic tissue is slightly abnormal, with pancreatic acini and islets visible, and islets atrophy (as indicated by the black arrows). (B) Serum concentrations of AMS, D-LA and lipase were detected by ELISA. N=6. ****, P<0.0001. Each bar represents the mean ± SD of three independent experiments. $Power_{lipase}$ =0.98, $Power_{D\text{-}LA}$ =0.99, $Power_{AMS}$ =0.99. 4-week, acetic acid treatment for 4 weeks; 6-week, acetic acid treatment for 6 weeks; 8-week, acetic acid treatment for 8 weeks. AMS, amylase; Con, control group; D-LA, D-lactate; ELISA, enzyme-linked immunosorbent assay; HE, hematoxylin-eosin; IPAP, idiopathic pediatric acute pancreatitis; Mod, disease model group; SD, standard deviation.

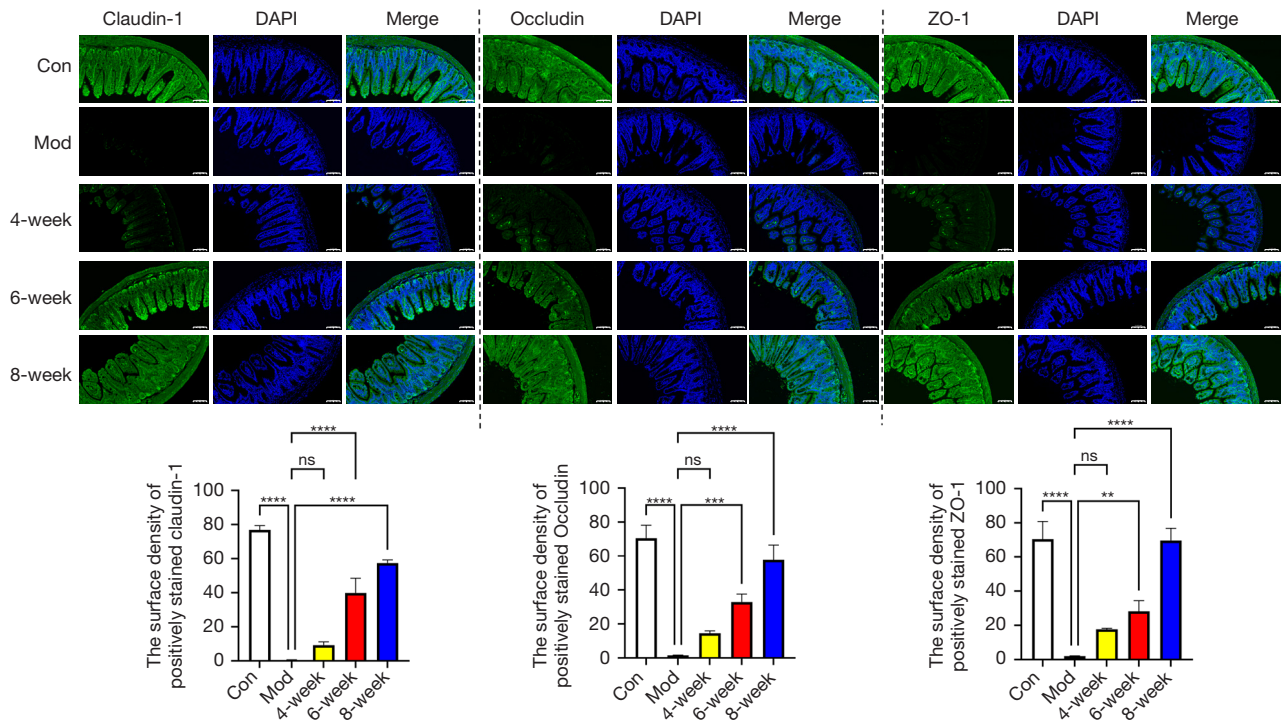

Figure 9 Immunofluorescence analysis of mouse ileum. N=3. ns, both ends of the horizontal line are not significant; **, P<0.01; ***, P<0.001; ****, P<0.0001. Each bar represents the mean ± SD of three independent experiments. $Power_{claudin-1}$ =0.65, $Power_{occludin}$ =0.64, $Power_{ZO-1}$ =0.64. The scale is 0.100 mm. 4-week, acetic acid treatment for 4 weeks; 6-week, acetic acid treatment for 6 weeks; 8-week, acetic acid treatment for 8 weeks. Con, control group; DAPI, 4',6-diamidino-2-phenylindole; IPAP, idiopathic pediatric acute pancreatitis; Mod, disease model group; SD, standard deviation.

group. *g_Monoglobus* is a common and representative AP-reducing species in AP studies, and is negatively correlated with liver function indicators (30). Among them, *Monoglobus pectinilyticus* is the first human intestinal bacteria found to degrade and utilize pectin, facilitated by high levels of pectin esterase and pectin lyase (31). *g_Dialister* is commonly found in the human intestine and exhibits both pathogenic and beneficial properties. In the study of colitis, the abundance of *g_Dialister* increased significantly following treatment, alongside elevated expression of cell regulatory factors MMP9, TGF-β and barrier proteins (claudin-1, occludin and ZO-1). This increase in *g_Dialister* abundance is beneficial for maintaining intestinal homeostasis (32).

Downstream metabolic regulation, centered on gut microbes, plays a direct role in disease progression. A significant correlation was observed between acetic acid and *g_Monoglobus*. *g_Monoglobus* may regulate the accumulation of acetic acid through genes and regulatory factors, and its mechanism is worth further exploration. In addition, serum (4E,15E)-bilirubin, D-fructose, and other substances are involved in the development of IPAP under the regulation of *g_Bacteroides*.

There are still some limitations in this study that need to be addressed. Due to the nature of the disease and the fit of the patients, case collection is a long-term process, so these experimental data are from a small number of children with IPAP. However, this study preliminarily clarified the metabolic characteristics of IPAP, providing a basis for etiological diagnosis and treatment. In the future, we will plan multi-center collaborations to obtain larger human sample studies to characterize the microbiome and metabolome, and to explore the therapeutic potential of acetic acid through controlled clinical trials. In addition, while human sample data provide valuable insights into the microbial and metabolic alterations associated with IPAP, intervention studies using mouse models may not be able to fully replicate the complexity of human disease. Nevertheless, the mouse model provides important mechanistic insights into the role of acetic acid in alleviating pancreatic and ileal damage, underlining its exploratory

nature and its role in guiding future clinical studies. Diet is also a well-known confounding factor, which can significantly affect the composition of the gut microbiota and the characterization of metabolites. While our study suggests that participants had similar eating habits, we cannot rule out the possibility that subtle differences in dietary intake may have influenced the results, and future studies should systematically collect and analyze dietary information using standardized assessment tools to better control for this confounder. Finally, we evaluated the potential of acetic acid to treat IPAP in a mouse model of AP, focusing on a relatively short period of time (4, 6, and 8 weeks), which demonstrated an acute effect of acetic acid intervention, consistent with the prominence of acetic acid in AP in previous studies (11,30,33), but the long-term effects of acetic acid therapy remain unclear. Next studies should extend the evaluation to 6–12 months and plan clinical trials in pediatric patients to determine the long-term therapeutic effect of acetic acid in improving outcomes.

Conclusions

In summary, our study provides information on the characteristic changes of IPAP gut microbes (*g_Monoglobus*, *g_Ruminococcus*, etc.), SCFAs (acetic acid, etc.), and serum metabolites (D-fructose, etc.) in human samples. The therapeutic effect of acetic acid was verified in a mouse model. The regulatory network formed by gut microbes influences IPAP development.

Acknowledgments

None.

Footnote

Reporting Checklist: The authors have completed the ARRIVE reporting checklist. Available at https://tp.amegroups.com/article/view/10.21037/tp-2024-571/rc

Data Sharing Statement: https://tp.amegroups.com/article/view/10.21037/tp-2024-571/dss

Peer Review File: Available at https://tp.amegroups.com/article/view/10.21037/tp-2024-571/prf

Funding: None.

Conflicts of Interest: All authors have completed the ICMJE uniform disclosure form (available at https://tp.amegroups.com/article/view/10.21037/tp-2024-571/coif). The authors have no conflicts of interest to declare.

Ethical Statement: The authors are accountable for all aspects of the work in ensuring that questions related to the accuracy or integrity of any part of the work are appropriately investigated and resolved. This study was conducted in accordance with the Declaration of Helsinki and its subsequent amendments. The Medical Ethics Committee of Tianjin Children's Hospital approved this study (No. W-2024-022) and waived the requirement for written informed consent, in line with local guidelines. The laboratory animal production license number is SCXK (Beijing) 2022-0006, and the laboratory animal qualification certificate number is 111423220100018067. The animal experiment was approved by the Animal Ethics Committee of Tianjin Jinke Bona Biotechnology Co., Ltd. (No. GENINK-20240020), and was performed in compliance with Chinese guidelines on animal care and use.

References

1. Husain SZ, Srinath AI. What's unique about acute pancreatitis in children: risk factors, diagnosis and management. Nat Rev Gastroenterol Hepatol 2017;14:366-72.
2. Schroeder BO, Bäckhed F. Signals from the gut microbiota to distant organs in physiology and disease. Nat Med 2016;22:1079-89.
3. Dike CR, Ollberding NJ, Thompson T, et al. Acute pancreatitis is associated with gut dysbiosis in children. Dig Liver Dis 2024;56:444-50.
4. Wang Z, Li F, Liu J, et al. Intestinal Microbiota - An Unmissable Bridge to Severe Acute Pancreatitis-Associated Acute Lung Injury. Front Immunol 2022;13:913178.
5. Li H, Xie J, Guo X, et al. Bifidobacterium spp. and their

metabolite lactate protect against acute pancreatitis via inhibition of pancreatic and systemic inflammatory responses. Gut Microbes 2022;14:2127456.
6. Wu L, Huang X, Ouyang Q, et al. Serum metabolomics study for acute attack of chronic pancreatitis. Clin Chim Acta 2023;541:117251.
7. Liu J, Wen B, Huang Y, et al. Exploring the effect of Clostridium butyricum on lung injury associated with acute pancreatitis in mice by combined 16S rRNA and metabolomics analysis. Anaerobe 2024;87:102854.
8. Xiong J, Liu Y, Lin X, et al. Geographic distance and pH drive bacterial distribution in alkaline lake sediments across Tibetan Plateau. Environ Microbiol 2012;14:2457-66.
9. Bolyen E, Rideout JR, Dillon MR, et al. Reproducible, interactive, scalable and extensible microbiome data science using QIIME 2. Nat Biotechnol 2019;37:852-7.
10. Callahan BJ, McMurdie PJ, Rosen MJ, et al. DADA2: High-resolution sample inference from Illumina amplicon data. Nat Methods 2016;13:581-3.
11. Lei Y, Tang L, Liu S, et al. Parabacteroides produces acetate to alleviate heparanase-exacerbated acute pancreatitis through reducing neutrophil infiltration. Microbiome 2021;9:115.
12. Peter TK, Withanage MHH, Comnick CL, et al. Systematic review and meta-analysis of oral squamous cell carcinoma associated oral microbiome. Front Microbiol 2022;13:968304.
13. Ai D, Pan H, Li X, et al. Association network analysis identifies enzymatic components of gut microbiota that significantly differ between colorectal cancer patients and healthy controls. PeerJ 2019;7:e7315.
14. Wang X, Shang Y, Wei Q, et al. Comparative Analyses of the Gut Microbiome of Two Fox Species, the Red Fox (Vulpes Vulpes) and Corsac Fox (Vulpes Corsac), that Occupy Different Ecological Niches. Microb Ecol 2022;83:753-65.
15. Chen Q, Ren R, Sun Y, et al. The combination of metagenome and metabolome to compare the differential effects and mechanisms of fructose and sucrose on the metabolic disorders and gut microbiota in vitro and in vivo. Food Funct 2023;14:7284-98.
16. Sugimura N, Li Q, Chu ESH, et al. Lactobacillus gallinarum modulates the gut microbiota and produces anti-cancer metabolites to protect against colorectal tumourigenesis. Gut 2021;71:2011-21.
17. Mann ER, Lam YK, Uhlig HH. Short-chain fatty acids: linking diet, the microbiome and immunity. Nat Rev Immunol 2024;24:577-95.
18. Niu J, Cui M, Yang X, et al. Microbiota-derived acetate enhances host antiviral response via NLRP3. Nat Commun 2023;14:642.
19. Sanchez-Lopez E, Zhong Z, Stubelius A, et al. Choline Uptake and Metabolism Modulate Macrophage IL-1β and IL-18 Production. Cell Metab 2019;29:1350-1362.e7.
20. York AG, Skadow MH, Oh J, et al. IL-10 constrains sphingolipid metabolism to limit inflammation. Nature 2024;627:628-35.
21. Hall B, Levy S, Dufault-Thompson K, et al. BilR is a gut microbial enzyme that reduces bilirubin to urobilinogen. Nat Microbiol 2024;9:173-84.
22. Zhou P, Chang WY, Gong DA, et al. High dietary fructose promotes hepatocellular carcinoma progression by enhancing O-GlcNAcylation via microbiota-derived acetate. Cell Metab 2023;35:1961-1975.e6.
23. Pan LL, Ren ZN, Yang J, et al. Gut microbiota controls the development of chronic pancreatitis: A critical role of short-chain fatty acids-producing Gram-positive bacteria. Acta Pharm Sin B 2023;13:4202-16.
24. Zhang Z, Huang J, Li C, et al. The gut microbiota contributes to the infection of bovine viral diarrhea virus in mice. J Virol 2024;98:e0203523.
25. Li XY, Zhu Y. Role of intestinal flora imbalance in intestinal mucosal barrier injury of acute pancreatitis. Chinese Journal of Practical Internal Medicine 2021;41:14-7.
26. Otsuka K, Isobe J, Asai Y, et al. Butyricimonas is a key gut microbiome component for predicting postoperative recurrence of esophageal cancer. Cancer Immunol Immunother 2024;73:23.
27. Wu Z, Sang L, Jiang M. Research advances in the inflammatory bowel disease dysbiosis. Chinese Journal of Practical Internal Medicine 2020;40:75-8.
28. Liu T, Liang X, Lei C, et al. High-Fat Diet Affects Heavy Metal Accumulation and Toxicity to Mice Liver and Kidney Probably via Gut Microbiota. Front Microbiol 2020;11:1604.
29. Cao Y, Oh J, Xue M, et al. Commensal microbiota from patients with inflammatory bowel disease produce genotoxic metabolites. Science 2022;378:eabm3233.
30. Liu J, Yan Q, Li S, et al. Integrative metagenomic and metabolomic analyses reveal the potential of gut microbiota to exacerbate acute pancreatitis. NPJ Biofilms Microbiomes 2024;10:29.
31. Kim CC, Lunken GR, Kelly WJ, et al. Genomic insights from Monoglobus pectinilyticus: a pectin-degrading specialist bacterium in the human colon. ISME J 2019;13:1437-56.

32. Feng Y, Chen S, Song Y, et al. A novel Sagittaria sagittifolia L. polysaccharides mitigate DSS-induced colitis via modulation of gut microbiota and MAPK/NF-κB signaling pathways. Int J Biol Macromol 2024;254:127835.
33. Wang J, Jiang M, Hu Y, et al. Lactulose regulates gut microbiota dysbiosis and promotes short-chain fatty acids production in acute pancreatitis patients with intestinal dysfunction. Biomed Pharmacother 2023;163:114769.

Cite this article as: Liu F, Sun Y, Wang J, Zhan J. Study on the pathogenesis of idiopathic pediatric acute pancreatitis by combining intestinal microbiome and metabolome. Transl Pediatr 2025;14(5):855-870. doi: 10.21037/tp-2024-571